JOURNAL OF MATERIALS SCIENCE 16 (1981) 2137–2144

Bonding mechanism between alumina and niobium

S. MOROZUMI, M. KIKUCHI, T. NISHINO
The Research Institute for Iron, Steel and Other Metals, Tohoku University, Sendai 980, Japan

Diffusion couples of Al_2O_3 single-crystal, sapphire, and Nb polycrystal were heat-treated in the temperature range 1873 to 2073 K under pressure in the range 3 to 15.2 MN m^{-2} for various times up to 3.6×10^3 sec. Tensile testing at various temperatures up to 1873 K in a vacuum of about 10^{-3} Pa, Knoop hardness testing at room temperature, optical microscopy, scanning electron microscopy, transmission electron microscopy, and electron-probe X-ray microanalysis studies were carried out on the specimens. From the results, it was concluded that the fairly high bond strength of a Al_2O_3–Nb interface might be attributed to the formation of a thin NbO_x layer, which had grown epitaxially on the Al_2O_3 surface. Lattice matching between Al_2O_3 and NbO_x phases was also considered.

1. Introduction

Alumina and niobium can easily be joined when they are kept in contact under a compressive load at an appropriate combination of temperature and time. Several works on the bonding properties have been reported [1–4]. Although the bonded interface between alumina and niobium has been observed by electron microscopy and analysed by X-ray diffraction techniques, the bonding mechanism is not completely understood. In the present work, transmission electron microscope observations were carried out around the bonded interface between the single-crystal alumina, the sapphire, and the niobium, in order to investigate the bonding mechanism between these two materials. Tensile testing was carried out to examine the bond strength, electron-probe X-ray microanalysis was undertaken to analyse the change of chemical composition across the interface, and hardness testing was carried out to study the diffusion of oxygen into the niobium matrix.

2. Experimental procedure

Two rods of single-crystal alumina of different diameters (2.8 and 6 mm), grown along the *c*-axis of the hexagonal lattice, were obtained from Kyoto Ceramic Ltd. The 2.8 mm diameter rod was sliced into 1 mm thick discs of (0001) plane surfaces, perpendicular to the *c*-axis, by using a multiwire saw, while the 6.0 mm diameter rod was cut into 2 mm thick discs in two ways: perpendicular and parallel to the *c*-axis to obtain (0 0 0 1) and (1 0 $\bar{1}$ 0) plane surfaces, respectively.

Niobium metal of 99.8% purity was electron-beam melted, swaged into a 8 mm diameter rod, and then machined to both screw-threaded and unthreaded disks of diameter 6 mm and thickness 4 mm. Each of the 2.8 mm diameter Al_2O_3 discs were sandwiched between two screw-threaded Nb discs, while each of the 6 mm diameter Al_2O_3 discs, of which the surface was either the (0001) or (1 0 $\bar{1}$ 0) plane, was bonded to two plain Nb discs under pressures in the range 3 to 15.2 MN m^{-2} for various times up to 2.88×10^4 sec (8 h) at temperatures in the range 1773 to 2073 K. Examples of bonded specimens are shown in Fig. 1a and b. The bonded screw-threaded specimens (Fig. 1a) were then tensile-tested at various temperatures up to 1873 K in a vacuum of about 10^{-3} Pa, except at room temperature, using an Instron-type machine at a cross-head speed of 1.3×10^{-6} m sec^{-1} (0.08 mm min^{-1}). The fractured surface was observed by optical and scanning

0022–2461/81/082137–08$02.80/0

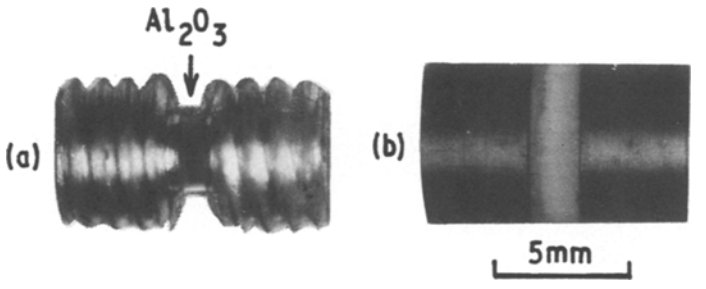

Figure 1 Values of Nb–Al_2O_3–Nb bonded specimens. (a) 2.8 mm diameter Al_2O_3–screw-threaded Nb disc specimen for tensile testing, and (b) 6.0 mm diameter Al_2O_3–plain Nb disc specimen for TEM, EPMA and X-ray study.

electron (SEM) microscopy techniques, as well as by electron-probe X-ray microanalysis (EPMA).

The bonded plain specimens (Fig. 1b) were sliced into 0.2 mm thick foils using a multiwire saw across the bonded interface, were then thinned down to about 60 μm in thickness by emery paper and then finally milled by the Micro Ion Mill, model MIM IV, in preparation for investigation by transmission electron microscopy (TEM), using a JEM 1000 electron microscope operated at 1000 kV.

EPMA was also performed across the Al_2O_3–Nb interface in order to examine the change of chemical composition in both materials, using a Shimazu EMX-SM2A machine, with a beam diameter of about 1.5 μm; the surface to be examined was coated with a carbon film 10 to 20 nm thick by a sputtering method to avoid the electric charging of the surface.

The Knoop hardness test with a load of 0.49 N was carried out on the same specimen as that used for EPMA examination to determine the hardness change across the interface.

3. Experimental results

Fig. 2 shows the variation of nominal bond strength with testing temperature for the specimens, heat-treated for 3.6×10^3 sec at 1873 K under a compressive stress of 8.8 MN m^{-2}. The bond strength decreases at temperatures above about 1100 K, at which temperature niobium becomes soft and very ductile. Above a temperature of about 1500 K, remarkable deformation in the Nb-matrix near the bonded interface took place prior to fracture.

The variation of bond strength with the bonding pressure at which the specimens were maintained for 3.6×10^3 sec at 1873 K is shown in Fig. 3. At 15.2 MN m^{-2} the Nb discs deformed a little; this pressure marked the upper limit for bonding. Fig. 3 shows that the maximum attainable nominal bond strength in the present experiment was approximately 120 MN m^{-2}. The variation of bond strength with treatment temperature for the specimens bonded under a pressure of 6.4 MN m^{-2} for 3.6×10^3 sec showed that

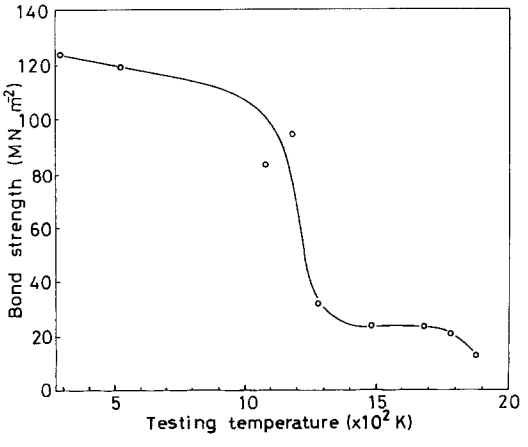

Figure 2 Variation of bond strength of Al_2O_3–Nb bond with testing temperature for the specimen heat-treated for 3.6×10^3 sec at 1873 K under a stress of 8.8 MN m^{-2}.

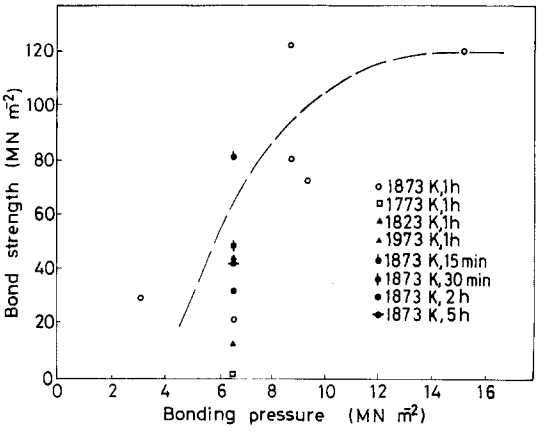

Figure 3 Variation of bond strength of Al_2O_3–Nb bond with bonding pressure for the specimens heat-treated for 3.6×10^3 sec 1873 K, together with treatment temperature and time dependence of bond strength for the specimen subjected to a stress of 6.4 MN m^{-2}.

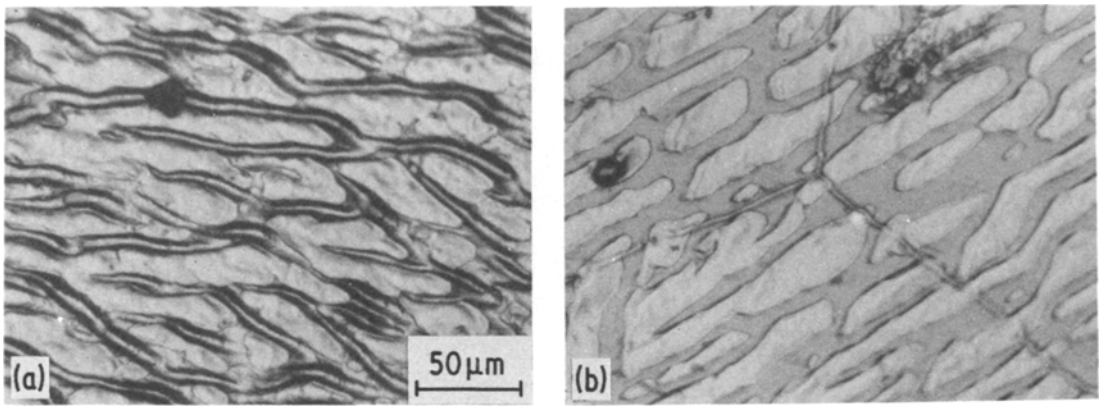

Figure 4 Photomicrographs of torn surfaces of the specimen heat-treated for 3.6×10^3 sec at 1873 K under a stress of 6.4 MN m^{-2}, followed by further treatment for 1.44×10^4 sec at 1873 K under no stress and then tensile tested at room temperature: (a) Al_2O_3 and (b) Nb surface.

the maximum bond strength was obtained at 1823 K, above which the bond strength decreased with treatment temperature in a way similar to that reported by Elssner *et al.* [2], and below which the bond strength decreased almost to zero (see Fig. 3).

Furthermore, the variation of bond strength with treatment time for the specimens heat-treated at 1873 K under a stress of 6.4 MN m^{-2} shows that only a very short time, typically 9×10^2 sec (15 min), is enough to bond the specimens, and that holding the specimens in contact for a long time does not necessarily contribute further to the bond strength (see Fig. 3).

The bond strength referred to above is the nominal strength, i.e. the ultimate strength per unit area of original section. However, the whole

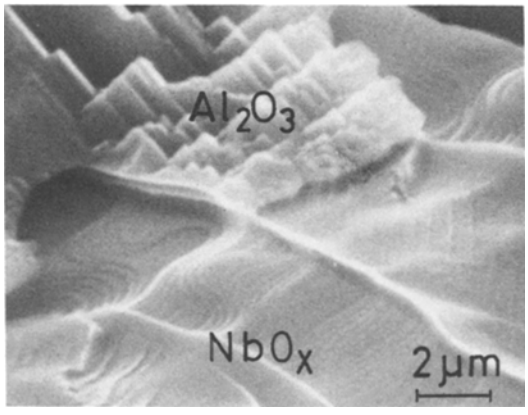

Figure 5 SEM micrograph of torn Nb (NbO_x) surface of the specimen heat-treated for 3.6×10^3 sec at 1973 K under a stress of 6.4 MN m^{-2} and tensile-tested at room temperature. Unbonded grooves can be seen.

of the Al_2O_3–Nb interface is not bonded so that the net bond strength should be larger than the nominal strength, as will be shown later.

In the tensile tests, all of the specimens fractured at the bonded interface. Fig. 4a and b illustrates photomicrographs of torn surfaces of the specimen bonded at 1873 K and tensile tested at room temperature, in which a network structure is seen on both surfaces. The network consists of grooves, where the surfaces are not joined with Al_2O_3 pieces remaining on the Nb surface, as seen in Fig. 5. Similar structure images from secondary electrons, taken by EPMA from torn surfaces on the same specimen as that shown in Fig. 4, are shown in Fig. 6, in which, again, Nb pieces can be seen to be remaining on the Al_2O_3 surface. As the pattern of the groove network does not depend on the grain orientation, that is, it does not change from grain to grain in the Nb matrix, as seen in Fig. 4b, and since it continues throughout the whole torn surface, it is deduced that the formation of the structure may strongly depend on the Al_2O_3 phase. The torn Nb surface in the specimen tensile tested at high temperatures above about 1500 K showed a dimple pattern, as illustrated in Fig. 7, because niobium could deform well (by up to a 50% reduction in area) at 1773 K before fracture took place.

The groove network was not clearly seen in the specimen treated for 3.6×10^3 sec at 1873 K under a stress of 8.8 MN m^{-2} and tensile tested below about 1600 K, while such a network was seen in the specimen treated at the same temperature and time but under a stress of 6.4 MN m^{-2} and tensile tested at room temperature. This fact may suggest

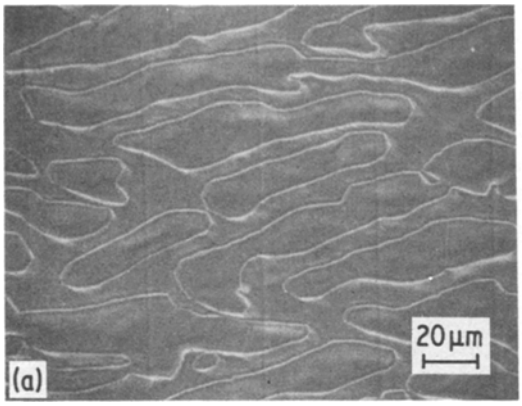

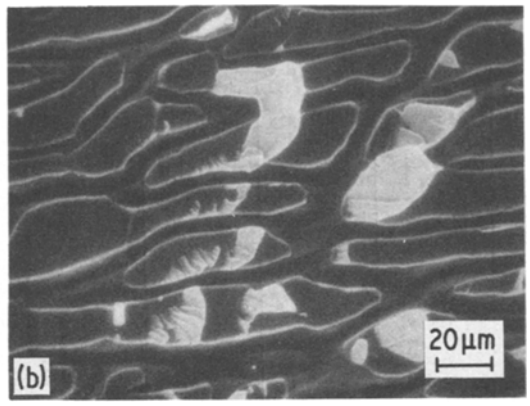

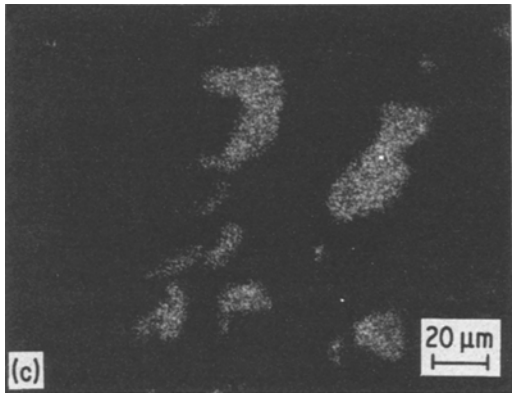

Figure 6 EPMA pictures for torn Al_2O_3 and Nb surfaces of the same specimen as that shown in Fig. 4. Secondary electron images of (a) Nb, and (b) Al_2O_3 surfaces; Nb Lα X-ray image (c) of the Al_2O_3 surface.

that the appearance of the groove structure depends on the heat-treating and testing conditions, and that probably a higher-treating temperature or a lower compressive load would produce a more developed groove network.

As mentioned above, the whole Al_2O_3–Nb interface was not bonded but formed a groove network. Furthermore, the circumferential area of the interface was also not bonded in an outside region less than 100 μm from the edge, because of thermal etching of the Al_2O_3 surface. As a result, the average area bonded was about 47%. Therefore, for instance, the net bond strength for a nominal strength of 122 MN m^{-2} becomes about 260 MN m^{-2}, which is less than the ultimate tensile strength, about 300 MN m^{-2}, but appreciably higher than the yield strength, about 200 MN m^{-2}, of niobium.

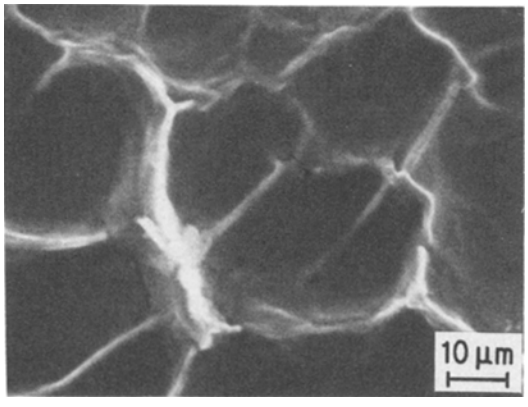

Figure 7 A dimple pattern on the torn Nb surface of the specimen heat-treated for 3.6×10^3 sec at 1873 K under a stress of 8.8 MN m^{-2} and tensile tested at 1683 K.

Fig. 8 is a typical photomicrograph of a thin foil prepared for TEM by ion milling. A thin reaction layer of about 20 μm, formed by heat-treating for 3.6×10^3 sec at 1973 K under a stress of 6.4 MN m^{-2}, is observed; at the Al_2O_3–reaction layer boundary several cavities are seen, which correspond to the sections of grooves. The thickness of the layer corresponds well to the diffusion zone in EPMA, as seen in Fig. 9, in which it is found that aluminium and especially oxygen can diffuse deeply into the Nb phase, while niobium can diffuse only slightly into the Al_2O_3 phase. The former diffusion zone in the Nb phase can be regarded to correspond to the reaction layer in Fig. 8. The thickness of the layer obtained from data of EPMA increases with heat-treatment time and/or temperature up to 1973 K, as shown in Figs 10 and 11.

Fig. 12 shows the changes of Knoop hardness in the Nb matrix with distance from the Al_2O_3–Nb interface in the specimens treated for various times at 1873 K and for 3.6×10^3 sec at 1973 K under a stress of 6.4 MN m^{-2}. The hardness decreases with

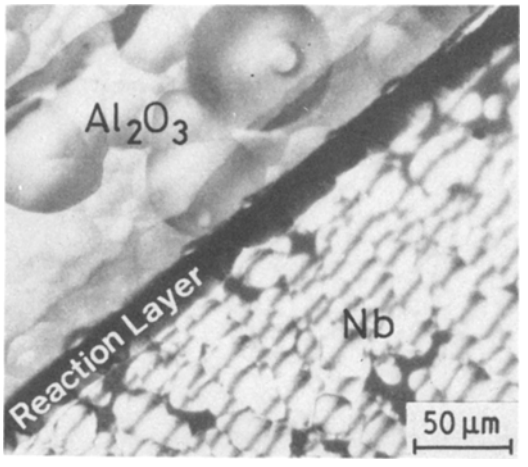

Figure 8 Photomicrograph of a thin foil prepared for TEM by ion milling. A reaction layer (NbO_x) can be seen between the Al_2O_3 and Nb.

distance, but remains at a higher level over a relatively longer distance than that seen in the original Nb matrix, and the level increases with both treatment time and temperature.

Fig. 13 shows an example of TEM photomicrographs of the boundary between the (0 0 0 1) plane of the Al_2O_3 phase and the reaction layer. A strain-field image is seen in the Al_2O_3 phase adjacent to the boundary, which may be attributed to the lattice mismatch between the two phases. The accompanying electron diffraction patterns show that the crystal structure of the reaction layer is body-centered tetragonal and is identified as NbO_x with lattice parameters $a_0 = 0.3395$ nm, $c_0 = 0.3276$ nm, and $a_0/c_0 = 1.0363$ [5]. The patterns also show that there are the following orientation relations between the Al_2O_3 phase and the NbO_x phase:

$$[\bar{2}\,1\,1\,0]_{Al_2O_3} \parallel [3\,\bar{1}\,1]_{NbO_x}, \quad (1)$$

$$[0\,\bar{3}\,3\,0]_{Al_2O_3} \parallel [\bar{1}\,\bar{2}\,1]_{NbO_x}. \quad (2)$$

The latter relation, Relation 2, was also observed in the diffusion couple with the $(1\,0\,\bar{1}\,0)$ plane of Al_2O_3. Lattice correspondence between the Al_2O_3 and NbO_x phases will be considered later.

The aspect of NbO_x–Nb boundaries is similar to that of grain boundaries in the Nb matrix, as illustrated in Fig. 14a and b. In Fig. 14a, a sub-boundary or dislocation network can be seen: the orientations of NbO_x and Nb, determined from the electron diffraction patterns, are the same. In this area, the tetragonality of the NbO_x lattice is very small and the lattice parameters of both phases are almost the same. In Fig. 14b, the plane of the photograph is the $(1\,1\,0)_{NbO_x}$ and $(1\,0\,0)_{Nb}$, and a large-angle boundary is seen between these two phases.

4. Discussion

As mentioned above, the reaction layer of NbO_x was formed between Al_2O_3 single crystal and Nb polycrystal. This NbO_x layer is also a single crystal and was determined to have Relations 1 and 2 with the Al_2O_3 phase. Relation 1, obtained by the electron diffraction analysis of a thin foil, involves an unavoidable uncertainty in the determination of the surface orientation of foil; on the other hand, Relation 2 is more accurate. Therefore, the lattice matching between $(0\,0\,0\,1)_{Al_2O_3}$ and $(0\,1\,2)_{NbO_x}$ is constructed as shown in Fig. 15, based on

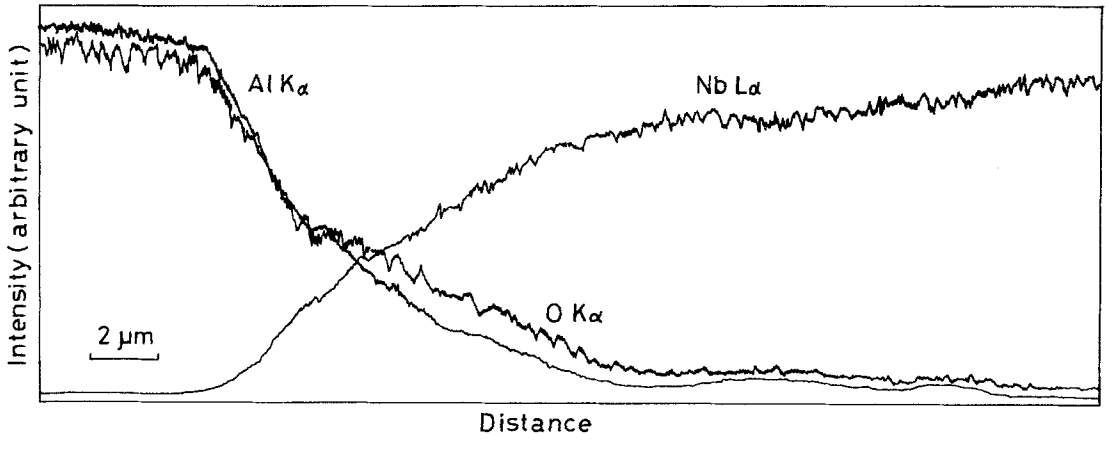

Figure 9 Concentration profile by EPMA across the Al_2O_3–Nb interface of the specimen heat-treated for 3.6×10^3 sec at 1973 K under a stress of 6.4 MN m^{-2}.

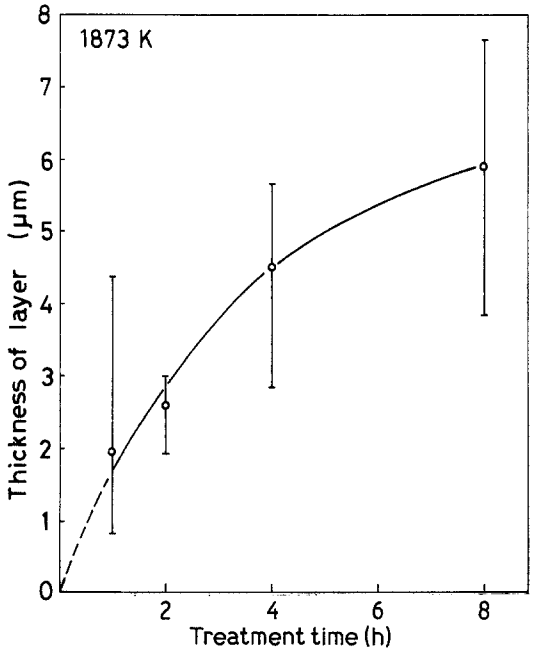

Figure 10 Variation of thickness of reaction layer with treatment time for the specimen tested at 1873 K under a stress of 6.4 MN m^{-2}.

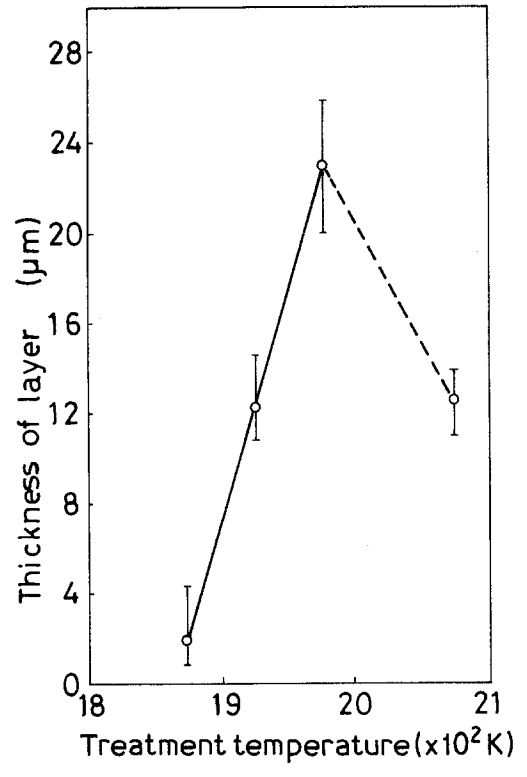

Figure 11 Variation of thickness of reaction layer with treatment temperature for the specimen treated for 3.6×10^3 sec under a stress of 6.4 MN m^{-2}.

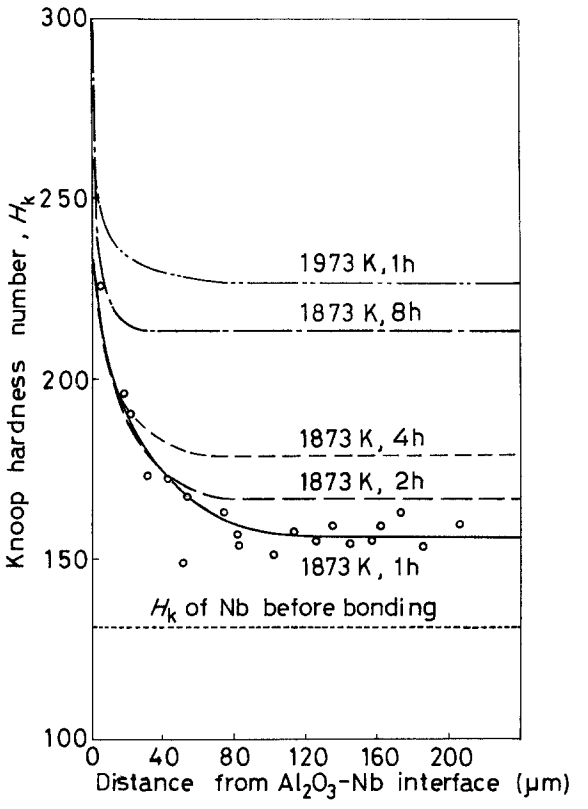

Figure 12 Variation of Knoop hardness with distance from the Al_2O_3–Nb interface in the Nb matrix for the specimens treated for various times at 1873 K and for 3.6×10^3 sec at 1973 K under a stress of 6.4 MN m^{-2}.

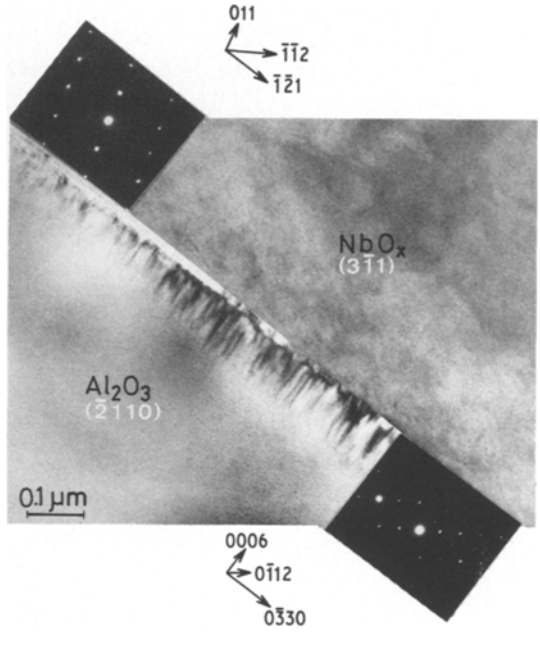

Figure 13 TEM photomicrograph of the Al_2O_3–NbO_x boundary region.

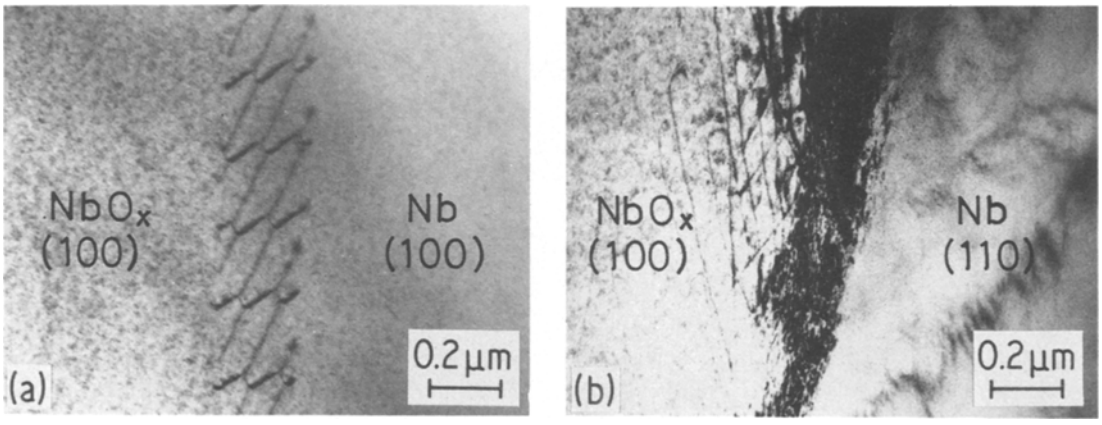

Figure 14 TEM photomicrographs in the region of the NbO_x–Nb boundary: (a) $(1\,0\,0)_{NbO_x} \parallel (1\,0\,0)_{Nb}$; (b) $(1\,0\,0)_{NbO_x} \parallel (1\,1\,0)_{Nb}$.

Relation 2 and referring to Relation 1. From the figure, in addition to Relation 2, the following relations can be established:

$$[0\,0\,0\,1]_{Al_2O_3} \parallel [0\,1\,2]_{NbO_x}, \quad (3)$$

$$[\bar{2}\,1\,1\,0]_{Al_2O_3} \parallel [5\,\bar{2}\,1]_{NbO_x}. \quad (4)$$

Relation 1 observed in the experiment is contradictory to Relations 3 and 4. However, the angle between $[3\,\bar{1}\,1]$ and $[5\,\bar{2}\,1]$ in NbO_x is only a few degrees, which can be regarded to be within the experimental error in determining the orientation of the thin foil by the electron diffraction analysis in TEM. Rotation of the NbO_x lattice around the $[\bar{1}\,\bar{2}\,1]$ axis by the angle, obeying Relation 2, can change the orientation of the foil from $(3\,\bar{1}\,1)$ to $(5\,\bar{2}\,1)$, and vice versa. Therefore, the rational

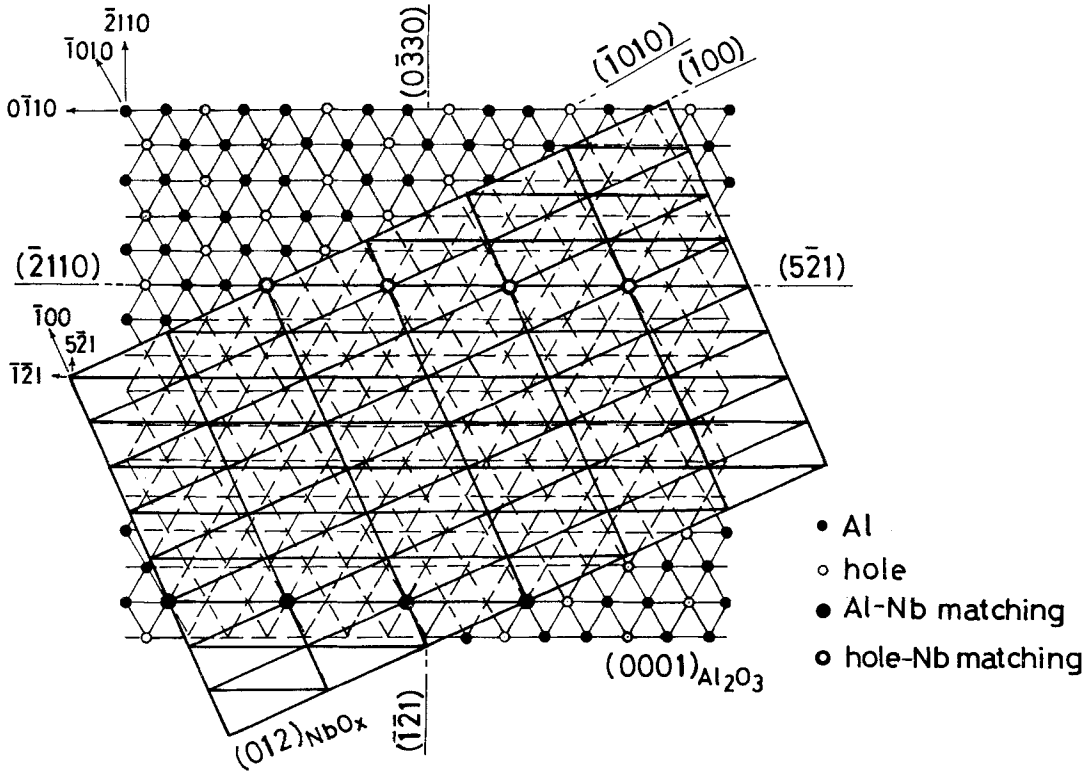

Figure 15 Lattice matching between parallel $(0\,0\,0\,1)_{Al_2O_3}$ and $(0\,1\,2)_{NbO_x}$ planes: the $(0\,1\,2)_{NbO_x}$ plane superimposed on the Al atom arrangement in $(0\,0\,0\,1)_{Al_2O_3}$ plane.

orientation of the NbO_x surface might be $[5\bar{2}1]$ rather than $[3\bar{1}1]$.

With Relations 2 to 4, the following crystal plane relations can be obtained along the same direction of $[0001]_{Al_2O_3}$ or $[012]_{NbO_x}$, which is perpendicular to the Al_2O_3–NbO_x interface:

$$(0001)_{Al_2O_3} \parallel (012)_{NbO_x}; \quad (5)$$

$$(0\bar{3}30)_{Al_2O_3} \parallel (\bar{1}\bar{2}1)_{NbO_x}; \quad (6)$$

$$(\bar{2}110)_{Al_2O_3} \parallel (5\bar{2}1)_{NbO_x}. \quad (7)$$

In Fig. 15, since the lattice parameters of $(0\bar{3}30)_{Al_2O_3}$ and $(\bar{1}\bar{2}1)_{NbO_x}$ are both equal to 0.1374 nm, good continuity between these two planes can be maintained, while in the direction of $[\bar{2}110]_{Al_2O_3}$ or $[5\bar{2}1]_{NbO_x}$, as the lattice parameters of $(\bar{2}110)_{Al_2O_3}$ and $(5\bar{2}1)_{NbO_x}$ are 0.2379 and 0.06191 nm, respectively, every ninth $(\bar{2}110)_{Al_2O_3}$ plane coincides with every 35th $(5\bar{2}1)_{NbO_x}$ plane within an error of about 1%. In the lattice matching between $(\bar{2}110)_{Al_2O_3}$ and $(5\bar{2}1)_{NbO_x}$, good continuity between $(0\bar{3}30)_{Al_2O_3}$ and $(\bar{1}\bar{2}1)_{NbO_x}$ is also maintained, while in the direction of $[0001]_{Al_2O_3}$ or $[012]_{NbO_x}$, every seventh $(0003)_{Al_2O_3}$ plane coincides with every twentieth $(012)_{NBO_x}$ plane within an error of 2%.

As a conclusion, it is deduced that when Al_2O_3 and Nb are kept in contact with each other at appropriate conditions of temperature, time and pressure, the NbO_x layer may grow epitaxially from the Al_2O_3 surface, depending on the orientation of Al_2O_3 and accompanying a thermal etching of the Al_2O_3 phase, and contributes to the bonding between Al_2O_3 and Nb. However, the thickness of the layer should be as small as possible for maximum bond strength between these two materials.

As the thermal expansion coefficients of Al_2O_3 and Nb are very close [2], any deformation due to the stress that results from the difference in the coefficient is not so large near the interface in the Nb phase.

5. Conclusions

Examining diffusion couples of Al_2O_3 single-crystal and Nb polycrystal, heat-treated at appropriate conditions under compressive stress, it was deduced that the bonding mechanism between them might arise from the formation of an NbO_x layer which could grow epitaxially from the Al_2O_3 surface, depending on the orientation of the surface, and that the thin layer of NbO_x might result in a greater bond strength.

Acknowledgements

The authors would like to thank Messrs S. Oki, F. Wagatsuma and T. Sato for help with the EPMA and X-ray measurements.

References

1. G. ELSSNER and G. PETZOW, *Z. Metallkde.* **64** (1973) 280.
2. G. ELSSNER, R. PABST and J. PUHR-WESTERHEIDE, *Z. Werkstofftechnik* 5 (1974) 61.
3. G. ELSSNER, S. RIEDEL and R. PABST, *Praktische Metallographie* **12** (1975) 234.
4. R. PABST and K. D. MÖRGENTBALER, *Z. Werkstofftechnik* 7 (1976) 62.
5. G. BRAUER, H. MÜLLER and G. KÜHNER, *J. Less-Common Metals* 4 (1962) 533.

Received 3 December 1980 and accepted 13 January 1981.